# MAGNETISM VIA SUPERCONDUCTIVITY IN SUPERCONDUCTOR—FERROMAGNET PROXIMITY STRUCTURES

V.N. KRIVORUCHKO, V.N. VARYUKHIN

Donetsk Institute of Physics and Technology, Nat. Acad. Sci. of Ukraine
*(72, R. Luxemburg Str., Donetsk 83114, Ukraine; e-mail: krivoruc@krivoruc.fti.ac.donetsk.ua)*

UDC 537.61:538.945


We consider the proximity effects in hybrid superconductor (S) — ferromagnet (F) structures drawing attention to the induced ferromagnetism of an S metal. The analysis is based on a quasiclassical theory of the proximity effect for metals under dirty limit conditions. It is shown that, below the superconducting critical temperature, ferromagnetic correlations extend a distance of order of the superconducting coherence length $\xi_S$ into a superconductor, being dependent on the S/F interface parameters. We argue that the properties of mesoscopic SF hybrids may drastically depend upon the magnetic proximity effect, and recent experiments lend support to the model of SF structures where the superconducting and magnetic parameters are tightly coupled.

## 1. Introduction

Proximity effects are phenomena stipulated by a "penetration" of an order parameter (of some state) from one material into another, which does not possess such a type of the order itself, due to the materials being in contact. The leakage of superconducting correlations into a non-superconducting material is an example of the superconducting proximity effect. For a nonmagnetic normal metal (N) in contact with a superconductor (S), the proximity effect has been intensively studied and well understood many years ago [1, 2]. However, in the case of SN structures, we deal with a single type of order — superconductivity. When a normal nonmagnetic metal is replaced by a ferromagnet (F), the proximity effect physics is much more interesting and rich [2—20]. There are two competing states with different order parameters: superconductivity and ferromagnetism. Due to the difference in energy between spin-up and spin-down electrons and holes under the exchange field of a ferromagnet, a singlet Cooper pair, adiabatically injected from a superconductor into a ferromagnet, acquires a finite momentum $\Delta p \sim H_e/\hbar v_{\rm F}$ (here $H_e = \mu_{\rm B} h_F$ is the extra energy caused by an intrinsic magnetic field $h_F$ in the ferromagnet; $v_{\rm F}$ is the Fermi velocity, $\hbar$ is the Planck constant, and $\mu_{\rm B}$ is the Bohr magneton). As a result, the proximity-induced superconductivity of the F layer is spatially inhomogeneous, and the order parameter contains nodes where the phase changes by $\pi$. Particularly, the transport properties of tunnel SF structures in the $\pi$-phase state have turned out quite unusual. The phase shift of $\pi$ in the ground state of the junction is formally described by the negative critical current $J_C$ in the Josephson current-phase relation: $J(\varphi) = J_C \sin(\varphi)$. The $\pi$-phase state of an SFS weak link due to a Cooper pair spatial oscillation was first predicted in [4, 5]. Experiments that have been performed by now on SFS weak links [6—8], and SIFS tunnel junctions [9] directly prove the $\pi$-phase superconductivity (I denotes an insulator). Planar tunneling spectroscopy also reveals a $\pi$-phase shift in the order parameter, when superconducting correlations coexist with the ferromagnetic order [10]. The superconducting phase was also measured directly [11] using SQUIDs made of $\pi$-junctions.

There is another interesting case of a thin F layer, $d_F \ll \xi_F$, being in contact with an S layer. As far as the thickness of the F layer, $d_F$, is much less than the corresponding superconducting coherence length, $\xi_F$, there is the spin spiltting, but there is no order parameter oscillation in the F layer. Surprisingly, but it was recently predicted in [12, 13] that, for SFIFS tunnel structures with very thin F layers, one can turn the junction into the $\pi$-phase state with the critical current inversion if there is a parallel orientation of the magnetizations of F layers; if there is the antiparallel orientation of the internal fields of F layers, one can even enhance the tunnel current. It was shown in [14, 15], that the physics behind the inversion and the enhancement of the supercurrent differs in this case from that proposed in [4, 5].

Whereas the proximity-induced superconductivity of an F metal in SF hybrid structures has been intensively studied, a much lesser attention has been paid to a modification of the electron spectrum of

a superconductor in a region near the S/F interface due to a leakage of magnetic correlation into the superconductor. Some features of the induced magnetism (e.g., the spin-splitting of the density of states) were found by numerical calculations in [16—18]. To our knowledge, only recently the question of S metal magnetization has been addressed in [19, 20]. (Here, we do not touch S/FI systems, where FI stands for a ferromagnetic insulator (semiconductor). In such systems, conduction electrons penetrate the magnetic layer on much smaller distances than in the case of metals and are totally reflected at the S/FI boundary. The S/FI boundary being magnetically active rotates spins of reflected electrons. This spin rotation occurs only as a result of the tunneling by a quasiparticle into the classically forbidden region of the boundary. Due to the spin rotation, the exchange field is induced in a superconductor on a distance of the order of the superconducting coherence length $\xi_S$ near the S/FI surface [21—23]. However, in contrast to ferromagnetic metals, where the proximity effect is pronounced, this effect is drastically reduced in S/FI structures.)

The investigation of the "magnetic proximity" effect in SF nanostructures is the purpose of this report. To tackle the physics, we consider an interesting and practicable case of the SF structure of a massive superconducting and thin ferromagnetic layers. Using a quasiclassical theory of superconductivity for a proximity-coupled bilayer (Section 2), we will show that for some limits the problem can be solved analytically. Two limits will be discussed here: (i) the weak and (ii) strong proximity effects. Section 3 is the key one; here, we describe the examples of the magnetic proximity effect manifestation. We show that, due to the induced magnetism of an S metal: (i) the superconducting phase jumps at the S/F interface; as well as, there are (ii) additional suppression of the order parameter near the S/F interface; (iii) the spin splitting of the quasiparticle density of states (DOS); (iv) the appearance of local bands inside the energy gap; and, directly, (v) the induced equilibrium electronic magnetization of the S layer that spreads over a distance of the order of the superconducting coherence length $\xi_S$. We also briefly discuss recent experiments. Summarizing the results in Conclusion, we draw attention to the fact that, in the general case for proximity-coupled SF hybrid structures, both phenomena — the induced superconductivity of the F metal and the induced magnetism of the S metal — take place simultaneously and should be considered self-consistently.

## 2. Quasiclassical Theory of Superconductivity of an SF Bilayer

### 2.1. Bilayer model

Let us consider proximity effects in the bilayer of a massive superconducting metal ($d_S \gg \xi_S$) and a thin ferromagnetic ($d_F \ll \xi_F$) one, with arbitrary transparency of the S/F interface. Here, $\xi_S = (D_S/2\pi T_C)^{1/2}$ and $\xi_F = (D_F/2H_e)^{1/2}$ stand for the superconducting coherence lengths, $D_{S,F}$ are the diffusion coefficients, $d_{S,F}$ are the thicknesses of the S and F layers. (Henceforth, we have taken the system of units with $\hbar = k_B = 1$.) We assume the "dirty" limit for both metals, i.e., $\xi_{S,F} \gg l_{S,F}$ where $l_{S,F}$ are the electron mean free paths. It is also assumed that the superconducting critical temperature of the F material equals zero. All quantities are assumed to depend only on a single coordinate $x$ normal to the interface surface of the materials. We also expect that the F layer has a homogeneous (monodomain) magnetic structure with magnetization aligned in parallel to the interface, so that there is no spontaneous magnetic flux penetrating into the S layer. Under these conditions, the only magnetic interaction which can affect the superconductor is the short-range exchange interaction between superconducting quasiparticles and magnetic moments into the ferromagnet.

### 2.2. Main equations

As is well known, the superconductivity of 'dirty' metals is conveniently described by the quasiclassical Usadel equations [24] for the normal, $G_{\sigma\sigma'}(x,\omega)$ and $\widetilde{G}_{\sigma\sigma'}(x,\omega)$, and anomalous, $F_{\sigma\sigma'}(x,\omega)$ and $\widetilde{F}_{\sigma\sigma'}(x,\omega)$, Green functions integrated over energy and averaged over the Fermi surface. (Green functions are defined in the standard way, see, e.g. [25]). It can be shown that, for the singlet pairing and in the absence of spin-flip scattering, the whole system of Usadel equations decomposes into two equivalent subgroups which pass into each other under the interchange of spin indices ($\sigma = \uparrow, \downarrow$) $\uparrow \longleftrightarrow \downarrow$ and reversal of the exchange field sign, $H_e \longleftrightarrow -H_e$

It is convenient to take into account explicitly the normalization of the Green function, $G_{F\uparrow\uparrow}\widetilde{G}_{F\downarrow\downarrow} + F_{F\downarrow\uparrow}F^{+}_{F\uparrow\downarrow} = 1$, and to introduce [2] modified Usadel

functions $\Phi_S$, $\Phi_F$ defined by the relations $\Phi_S = \omega F_S/G_S$, $\Phi_F = \tilde{\omega} F_F/G_F$, etc. Then we can recast the equations for the S layer in terms of these functions. We specialize the discussion to a geometry when all quantities depend on a single coordinate $x$ normal to the S/F interface. For the superconducting metal, we have ($x \geq 0$)

$$\Phi_S = \Delta_S + \xi_S{}^2 \frac{\pi T_C}{\omega G_S}[G_S{}^2 \Phi_S']',$$

$$G_S = \frac{\omega}{(\omega^2 + \Phi_S \tilde{\Phi}_S)^{1/2}} \tag{1}$$

with the superconducting order parameter $\Delta_S(x)$ determined by the self-consistency equation

$$\Delta_S \ln(T/T_C) + 2\pi T \sum_{\omega>0} [(\Delta_S - \Phi_S G_S)/\omega] = 0. \tag{2}$$

Here, the prime denotes the differentiation with respect to the coordinate $x$, and the summation over frequencies in Eq. (2) is cut off by the Debye frequency $\omega_D$. For the F metal, we have ($-d_F \leq x < 0$)

$$\Phi_F = \xi^2 \frac{\pi T_C}{\tilde{\omega} G_F}[G_F{}^2 \Phi_F']', \qquad G_F = \frac{\tilde{\omega}}{(\tilde{\omega}^2 + \Phi_F \tilde{\Phi}_F)^{1/2}}. \tag{3}$$

Here, $\tilde{\omega} = \omega + iH_e$, and $\omega \equiv \omega_n = \pi T(2n+1)$, $n = \pm 1, \pm 2, \pm 3, ...$ is the Matsubara frequency. Assuming the symmetry of the system with respect to a rotation in the spin space both in the F and S layers, we drop the spin indices apart from the specified cases. We also put a vanishing value of the bare superconducting order parameter $\Delta_F = 0$ for the F metal, whereas the pair amplitude $F_F \neq 0$ due to the proximity with the superconductor.

The equations for the functions $\tilde{\Phi}_S$ and $\tilde{\Phi}_F$ have a form analogous to (1)—(3); note that $\tilde{\Phi}(\omega, H_e) = \Phi^*(\omega, -H_e)$. In Eq. (3), we write our formulas for the F metal using the effective coherence length of a normal nonmagnetic (N) metal with the diffusion coefficient $D_F$, $\xi = (D_F/2\pi T_C)^{1/2}$, instead of $\xi_F = (D_F/2H_e)^{1/2}$, to have a possibility to analyze both limits $H_e \to 0$ (SN bilayer) and $H_e \gg \pi T_C$. The relation for the ferromagnetic layer thickness may read as $d_F \ll \min(\xi_F, \xi)$.

### 2.3. Boundary conditions

Equations (1)—(3) should be supplemented with the boundary conditions in the bulk of the S metal and at the external surface of the F layer. Far from the S/F interface, $x \gg \xi_S$, for the S layer, we have the usual boundary conditions in the bulk of the S metal: $\Phi_S(\infty) = \Delta_S(\infty) = \Delta_0(T)$, where $\Delta_0(T)$ is the BCS value of the order parameter. At the external surface of the F metal, $\Phi_F'(-d_F) = 0$. The relations at the S/F interface were obtained [26] by generalizing the results in [27] for an interface between two superconductors.

The first condition on the Usadel equations ensures the continuity of the supercurrent flowing through the S/F boundary at any value of the interfacial transparency. Going over to the modified Usadel functions $\Phi_S$ and $\Phi_F$, the first boundary condition has the form

$$\frac{1}{\tilde{\omega}} \gamma \xi G_F{}^2 \Phi_F'\Big|_{x=0} = \frac{1}{\omega} \xi_S G_S{}^2 \Phi_S'\Big|_{x=0}. \tag{4}$$

Here, $\gamma = \rho_S \xi_S/\rho_F \xi$ is the proximity effect parameter which characterizes the intensity of superconducting correlations induced in the F layer and, vice versa, the intensity of magnetic correlations induced into the S layer; $\rho_{S,F}$ are the resistivities of the metals in the normal state.

The boundary condition (4) takes into account the effect of quasiparticle DOS of the metals in contact. The second relation takes into consideration the effects of a finite transparency (electrical quality) of the interface. For the $\Phi(\omega, x)$-parametrization, the second boundary condition becomes

$$\xi \gamma_{BF} G_F \Phi_F'|_{x=0} = \tilde{\omega} G_S (\Phi_S/\omega - \Phi_F/\tilde{\omega})|_{x=0}, \tag{5}$$

where $\gamma_{BF}$ is the parameter that characterizes the effects of a finite transparency of the interface. For $\gamma_{BF} = 0$, i.e., for a fully transparent boundary, condition (5) passes to $\Phi_S/\omega = \Phi_F/\tilde{\omega}$. The expression for $\gamma_{BF}$ can be written through more convenient values: $\gamma_{BF} = R_B/\rho_F \xi$, where $R_B$ is the product of the S/F boundary resistance and its area [27].

Relations (4) and (5) generalize the proximity effect problem with an arbitrary interface transparency for the case of a normal metal with ferromagnetic order. The additional physical condition we assumed is that the exchange splitting of the momentum subbands, $p_F^{\pm} = \sqrt{2m}\sqrt{E_F \pm H_e}$, is substantially smaller than the Fermi energy $E_F$ ($m$ is the effective mass of an electron). For most magnetic materials, the momentum renormalization is not so important as the frequency renormalization, because $H_e \gg \omega_n \sim \pi T_C$ while $H_e \ll E_F$. Due to this fact, the differences in the DOS and transparencies of the S/F interface for electrons with opposite spin orientations can be neglected.

According to the Green functions formalism, if the functions $G_{S,F}(x, \omega)$ and $F_{S,F}(x, \omega)$ are known, that is

all we need to be able to describe, at least in principle, any superconducting and magnetic properties of the system. We draw attention to the feature important for further conclusions: due to superconductivity, it is only a single space length — the respective superconducting coherence length, $\xi_S$ or $\xi_F$, — that encounters into the differential equations (1) and (3). So, due to superconductivity, the coordinate dependences of both superconducting and magnetic properties of each layer have the same typical space scale.

### *2.4. Analytical solutions*

The proximity effect for an SF structure with a thin F metal, $d_F \ll (\xi_F, \xi)$, can be reduced to the consideration of the boundary-value problem for the S layer [2, 26, 28]. Indeed, the differential equation (3) can be solved by iteration with respect to the parameter $d_F/\xi_F$ ($d_F/\xi$). In the first approximation, we can neglect the nongradient term and, taking into account that $\Phi_F^{'}(-d_F) = 0$, we obtain $\Phi_F(x) = const$. In the next approximation in $d_F/\xi$, we find, after linearizing Eq.(3),

$$\Phi_F(\omega, x) = \frac{\tilde{\omega}\Phi_F(\omega, 0)}{\xi\pi T_C G_F}\,(x + d_F)\,. \tag{6}$$

Here, we have again taken into account the condition that $\Phi_F^{'}(-d_F) = 0$. Determining $\Phi_F^{'}(0)$ from Eq. (6) and substituting it into the boundary conditions (4) and (5), we obtain the boundary condition for the function $\Phi_S(\omega, x)$. We have (here, we restore the spin index)

$$\xi_S G_S \Phi_S^{'}|_{x=0} = \gamma_M \tilde{\omega}_\sigma \Phi_S \times$$

$$\times \left[\pi T_C \left(1 + \frac{2G_S\gamma_B\tilde{\omega}_\sigma}{\pi T_C} + \frac{(\gamma_B\tilde{\omega}_\sigma)^2}{(\pi T_C)^2}\right)^{1/2}\right]^{-1}|_{x=0}, \tag{7}$$

where $\widetilde{\omega}_\sigma \equiv \omega + i\sigma H_e$. The unknown value of the function $\Phi_F(\omega, x = 0)$ is defined by the relation

$$\Phi_F(\omega, 0) = G_S\Phi_S\left[\omega\left(\frac{\gamma_B}{\pi T_C} + \frac{G_S}{\tilde{\omega}_\sigma}\right)\right]^{-1}|_{x=0}. \tag{8}$$

We introduce the effective boundary parameters, $\gamma_M = \gamma d_F/\xi$ and $\gamma_B = \gamma_{BF} d_F/\xi$, instead of $\gamma$ and $\gamma_B$. As a result, the problem of the proximity effect for a massive superconductor with a thin ferromagnet layer reduces to solving Eqs. (1) and (3) for a semi-infinite S layer with the boundary conditions (7) on the external side and those of the BCS type at infinity. The spatial dependence of the function $\Phi_F(\omega, x)$ in the F layer can be neglected due to the mesoscopic thickness $d_F \ll (\xi, \xi_F)$ of the latter; Eq. (8) determines the value of $\Phi_F(\omega, 0)$.

One can directly see that, via the boundary condition (7), the electron spin 'up' and spin 'down' subbands lost their equivalence in the S metal as well. *Spin discrimination means magnetism of a metal.* The penetration of the magnetic correlation into the superconducting layer is governed by the proximity effect parameter $\gamma_M$, i.e., by the electron density of states on contacting metals. For the high density of quasiparticles in the F metal in comparison to that in the S counterpart (a large value of $\gamma_M$), the equilibrium diffusion of these quasiparticles into the superconductor leads to the effective leakage of a magnetic order into the S layer and the strong suppression of superconductivity near the S/F interface. In the opposite case, $\gamma_M \ll 1$, the influence of the F layer on properties of the S metal is weak; it even vanishes if $\gamma_M \longrightarrow 0$. Opposite is the behavior of the superconductivity upon a variation of this parameter. So, to increase the magnetic correlation near the S/F interface, one should increase the parameter $\gamma_M$; in order to increase the superconducting correlation, one should decrease this parameter. Of course, the electric quality of the interface is also important for the penetration of magnetic and superconducting correlations from one metal into another.

There are three parameters which enter the model: $\gamma_M$ is the measure of the strength of the proximity effect between $S$ and $F$ metals, $\gamma_B$ describes the electrical quality of the SF boundary, and $H_e$ is the exchange correlation energy in the $F$ layer. In the general case, the problem needs a self-consistent numerical solution. Here, to consider the new physics we are interested in, we will not discuss the quantitative calculations, but will use analytical ones obtained earlier in [26, 28] for two limits: (a) $\gamma_M \ll 1$, a small strength of the proximity effect — a low suppression of the order parameter in the S layer near the S/F boundary, and (b) $\gamma_M \gg 1$, a strong suppression of the order parameter in the S layer near the S/F boundary. Note that the results obtained are applicable to any value of the S/F boundary transparency, as we make no specific assumption about $\gamma_B$ in the derivation given below.

*Weak proximity effect.* If $\gamma_M \ll 1$, we can find the explicit expression

$$\Phi_S(\omega, x) = \Delta_0\left\{1 - \gamma_M\beta\tilde{\omega}\frac{\exp(-\beta x/\xi_S)}{\gamma_M\beta\tilde{\omega} + \omega A(\omega)}\right\}, \tag{9}$$

where $\beta = [(\omega^2 + \Delta_0^2)/\pi T_C]^{1/2}$ and $A(\omega) = \left[1 + \gamma_B\tilde{\omega}\left(\gamma_B\tilde{\omega} + 2\omega/\beta^2\right)/(\pi T_C)^2\right]^{1/2}$. As one can expect, the magnetic correlation spreads into the S film

over a distance of about $\xi_S$, and it can much exceed the distance of the superconducting correlation spreading into the F film $\xi_F$. If $H_e \longrightarrow 0$ (i.e., $\tilde{\omega} \longrightarrow \omega$), result (9) restores with that for the SN bilayer in the limit in question (see, e.g., [2]). For the function $\Phi_F(\omega, 0)$, we obtain

$$\Phi_F(\omega, 0) = \Delta_0 \tilde{\omega}_S / (\gamma_B \tilde{\omega} \beta^2 + \omega).$$

*Strong proximity effect.* When $\gamma_M \gg 1$, the behavior of $\Phi_S(\omega, x)$ near the S/F boundary, $0 < x \ll \xi_S$, is given by

$$\Phi_S(\omega, 0) = B(T)\{(\pi T_C + \gamma_B \tilde{\omega})/\gamma_M \tilde{\omega}\} \qquad (10)$$

Here, $B(T) = 2T_C[1 - (T/T_C)^2][7\zeta(3)]^{-1/2}$ (see [2]) and $\zeta(3) \cong 1.2$ ($\zeta$ is the Riemann function). In this approximation,

$$\Phi_F(\omega, 0) = B(T)\pi T_C/\gamma_M \omega.$$

It is seen that the proximity-induced superconductivity in the F layer is independent of the boundary transparency, but decreases with increase in $\gamma_M$. To obtain the results for larger distances, $x \gtrsim \xi_S$, the equations should be solved numerically by a self-consistent procedure. We will not discuss these results here.

## 3. Manifestation of the Magnetic Proximity Effect

An important feature of the results obtained for the SF structure is that the modified Usadel function for the S layer $\Phi_S(\omega, x)$, Eqs. (9) and (10), directly depends on the exchange field of an F metal. That is the reason to speak about the exchange correlation that has been induced into the S layer due to superconductivity. In this section, we discuss a few examples of such a manifestation of the "magnetic proximity effect".

### *3.1. Phase variation at the SF interface*

Comparing the results for an SF structure with those for an SN bilayer, one can find a fundamental aspect that leads to new physical consequences; namely, $\Phi_S(\omega, x)$ is a complex function near the S/F interface. As a result, the additional 'superconducting phase rotation' (a phase jump on the S/F interface for our approximation of a thin ferromagnetic layer, $d_F \ll \xi_F$) occurs at the S/F interface. To illustrate this, let us take, for simplicity, a structure with the interface parameters favorable for magnetic effects: $\gamma_M \gg 1$ and $\gamma_B = 0$. Then, as follows from Eq. (10), the modified Usadel function at the S/F interface, $\Phi_S(\omega, 0)$, can be written as

$$\Phi_S(\omega, 0) = B(T)(\pi T_C/\gamma_M)\frac{\exp(-i\theta)}{(\omega^2 + H_e^2)^{1/2}} \qquad (11)$$

with $\theta = \arctan(H_e/\omega)$. Taking into account that a typical value of $\omega \sim \pi T_C$, one can see that, in the limit $H_e \gg \pi T_C$, the correlation function acquires an additional $\pm\pi/2$ phase shift in comparison with a similar function for the SN bilayer. For an SF multilayered system with strong enough ferromagnetism of the layers, the phase shift can be summarized or subtracted, depending on a mutual orientation of the magnetizations of F layers, leading to new effects in the superconductivity of SF hybrid structures. Namely, one can show that the proximity-induced magnetizm of S layers makes preferrable the $\pi$-phase superconductivity of the system for parallel directions of the exchange fields; for the antiparallel orientation of magnetizations and low temperature, the critical current can be even enhanced [12—15].

### *3.2. Suppression of the superconducting order parameter by an exchange field*

Another feature of the S/F boundary is that the gap $\Delta_S(x)$ is suppressed near the interface more strongly than that in the SN case. This is not surprising, since one would expect that the induced ferromagnetism suppresses the superconducting order parameter at some distance into the S layer in excess of that for a nonmagnetic normal layer. The suppression increases with the exchange energy $H_e$ and the electrical quality of the interface; far from the interface, $x \gg \xi_S$, the bulk superconductivity is restored.

Using $\Phi_S(\omega, x)$ (9) and the self-consistency condition (2), one can find a spatial variation of the order parameter in the $S$ layer $\Delta_S(x)$ for different values of $\gamma_B$ and $\gamma_M \ll 1$. The exchange interaction influence on the spatial variation of the order parameter in the S layer is shown in Fig. 1. Namely, the dependence of the difference of the order parameters for the case where the magnetic interaction is turned off (i.e., an SN bilayer) and with the ferromagnetic correlation (a SF bilayer) as function of the distance from the interface is shown; the boundary parameters, $\gamma_M$ and $\gamma_B$, are fixed. It is seen that the influence of magnetism decreases with increase in the distance from the S/F boundary. The scale, at which superconductivity reaches the value for a SN bilayer, is $\xi_S$ from the interface. The curves in Fig. 1 illustrate the spatial dependences of the induced

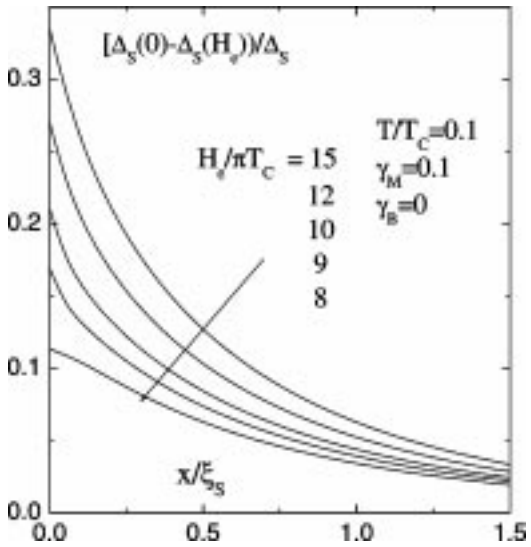


Fig. 1. Difference of the superconducting order parameter in the S layer versus the distance from the interface for SN and SF structures with the same boundary parameters ($\gamma_M = 0.1, \gamma_B = 0$) and different ferromagnetic field energies $H_e/\pi T_C$ = 8, 9, 10, 12 and 15

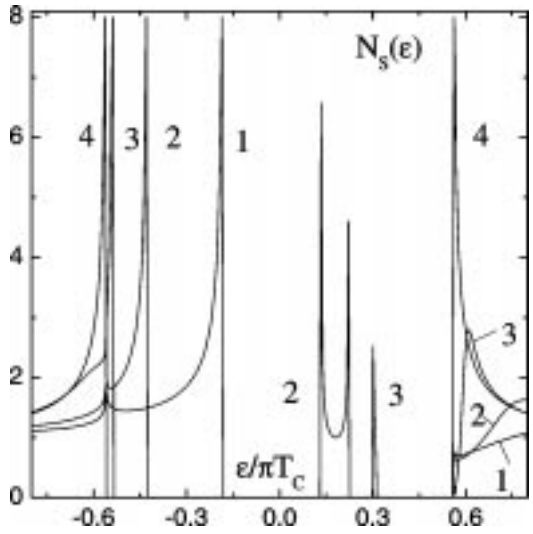


Fig. 2. Normalized density of state for spin 'up' quasiparticles in the S layer of the SF sandwich for $\gamma_M = 0.1$ , $\gamma_B = 0$ and $H_e = 5\pi T_C$, and various distances from the S/F interface: $x/\xi_S$ = 0, 1, 5, and 30 (curves *1, 2, 3,* and *4*, respectively)

exchange correlation in the superconductor for the case of vanishing interface resistance $\gamma_B = 0$. With increase in the SF boundary resistance, the electrical coupling of S and F metals decreases, and, in the limit $\gamma_B \longrightarrow \infty$, the metals become decoupled.

### *3.3. Exchange field spin-splitting of DOS and intra-gap states*

The spin splitting of the DOS and intergap states in the S layer are other manifestations of the magnetic correlation leakage into a superconductor. Note that the magnetic layer does not influence the DOS of the normal metal. In this case, the decay length is extremely small $\sim p_F^{-1} \simeq 1$ Å and the effect can be neglected.

The Green functions for the S layer $G_{S\uparrow\uparrow}(\omega, x)$ and $G_{S\downarrow\downarrow}(\omega, x)$ for both spin subbands can be obtained using the solutions for the functions $\Phi_S(\omega, x)$ with $\tilde{\omega} = \omega + iH_e$ and $\tilde{\omega} = \omega - iH_e$, respectively. Performing the analytical continuation to the complex plane by the substitution $\omega \rightarrow -i\varepsilon$ we calculate the spatial dependence of the quasiparticle DOS for the spin "up" and "down" subbands: $N_{S\uparrow}(\varepsilon, x) = \mathrm{Re}G_{S\uparrow\uparrow}(\omega, x)$ and $N_{S\downarrow}(\varepsilon, x) = \mathrm{Re}G_{S\downarrow\downarrow}(\omega, x)$, respectively. The total density of states for quasiparticles, by definition, is given by $N_S(\varepsilon, x) = N_{S\uparrow}(\varepsilon, x) + N_{S\downarrow}(\varepsilon, x)$. Using Eqs. (9) and (10), one can obtain the explicit expressions for the total DOS, as well as for a specified spin subband. The resulting expressions, which are cumbersome to be presented here, imply that, for $H_e \neq 0$, $\gamma_M \neq 0$, and $\gamma_B \neq 0$, the density of quasiparticle states is spin-splitted: $N_{S\uparrow}(\varepsilon, x) \neq N_{S\downarrow}(\varepsilon, x)$. This is because of the initial exchange field splitting of the Fermi surface in the F metal, which is manifested in the characteristics of the united system — the SF bilayer. The symmetry of the density of states with respect to the energy variable is also lost: $N_{S\uparrow}(\varepsilon > 0, x) \neq N_{S\uparrow}(\varepsilon < 0, x)$. However, as one can expect from the fermionic symmetry, spin-up particles and spin-down holes have the same DOS, as well as spin-down particles and spin-up holes. As a result, the total density $N_S(\varepsilon, x)$ is symmetric: $N_S(\varepsilon > 0, x) = N_S(\varepsilon < 0, x)$.

In Fig. 2, the representative $N_{S\uparrow}(\varepsilon, x)$ dependences at different distances from the S/F interface are presented for $H_e = 5\pi T_C$, $\gamma_M = 0.1$, and the vanishing boundary resistance ($\gamma_B = 0$). In Fig. 3, the same dependence is presented for $x/\xi_S = 1$ and different values of the exchange energy. We find that all features mentioned above are saved at a distance on the scale $\xi_S$ from the SF boundary. The spin splitting decreases with increase in the distance from the boundary and vanishes in the bulk of the S layer (see curve *4* in Fig. 2).

Other important features shown in Figs. 2 and 3 are the local states that appear inside the energy gap at distances up to a few $\xi_S$ from the S/F boundary. These intergap states are absent far from the S/F interface and

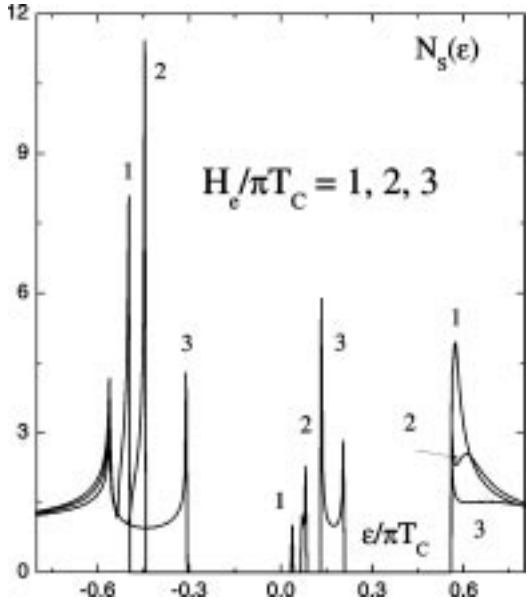


Fig. 3. Same as in Fig. 4 for $\gamma_M = 0.1$, $\gamma_B = 0.1$, $x = \xi_S$, and various ferromagnetic field energies: $H_e/\pi T_C = 1$, 2, and 5 (curves *1*, *2*, and *3*, respectively)

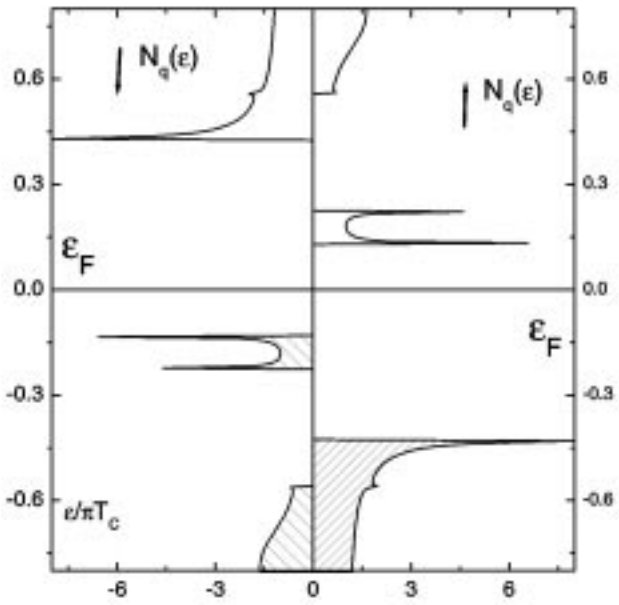


Fig. 4. Quasiparticle density of states in the S layer near the S/F interface; $\gamma_M = 0.1$, $\gamma_B = 0.0$, $x = \xi_S$, and $H_e = 5\pi T_C$. All states above Fermi energy are empty; all states below the Fermi level are filled (dashed regions)

if $H_e = 0$. For small values of $\gamma_M$ and $\gamma_B = 0$, relation (9) yields that $N_{S\uparrow}(\varepsilon, x)$ has a singularity for

$$\varepsilon = \pm\Delta_0\{1 - \frac{\gamma_M \beta_\varepsilon \tilde{\varepsilon}}{\varepsilon + \gamma_M \beta_\varepsilon \tilde{\varepsilon}} \exp(-\beta_\varepsilon x/\xi_S)\}, \qquad (12)$$

where $\beta_\varepsilon^2 = (\Delta_0^2 - \varepsilon^2)^{1/2}/\pi T_C$ and $\tilde{\varepsilon} = \varepsilon - H_e$. We found the singularity inside the superconducting gap, $-\Delta_0 < \varepsilon < \Delta_0$, by numerical calculations [19]. The local states are definitely not due to a spatial variation of the pair potential, but due to the breaking of Cooper pairs in the superconductor by the exchange-induced magnetic correlation. The region of their existence increases with $H_e$ or the pair breaking effects. In the absence of spin-flip (e.g., spin-orbit) scattering, the subgap bands accommodate quasiparticles with a definite ("up" or "down") spin direction. These bands bear a superficial resemblance to both the bands observed at the interface of a superconductor and a perfectly insulating ferromagnet [29] and a bulk superconductor containing finite concentrations of magnetic impurities [30, 31].

### *3.4. Induced magnetization of the S layer*

As we saw above, the influence of the ferromagnet on the superconductor is reflected in a nonzero value of the difference in the DOS for spin-up and spin-down unpaired electrons, $N_{S\uparrow}(\varepsilon, x)$ and $N_{S\downarrow}(\varepsilon, x)$. This DOS splitting causes an effective magnetization $M_S(x)$ of the S layer that can be found using the relation

$$M_S(x)/M_O = \int_0^\infty d\varepsilon\{N_{S\uparrow}(\varepsilon, x) - N_{S\downarrow}(\varepsilon, x)\}f(\varepsilon), \qquad (13)$$

where $M_O = gS_e\mu_B(= \mu_B)$ is a quasiparticle magnetic moment, $S_e = 1/2, g = 2$, and $f(\varepsilon) = 1/[\exp(\varepsilon/T) + 1]$ is the Fermi distribution function. Figure 4 illustrates the mechanism of the proximity-induced magnetization of the S layer. For $T < T_C$, we took $f(\varepsilon) = 1$, i.e., all states below the Fermi level are filled (dashed regions in Fig. 4), while all states above the Fermi energy are empty. One can directly see from the figure that the S layer acquires a nonzero magnetic moment. This suggestion is confirmed by numerical calculations of $M_S(x)$ (13) shown in Figs. 5, 6. Figure 5 shows the magnetization of the superconductor versus distance from the S/F interface for fixed boundary parameters. The same magnetic characteristics, but for an SF sandwich with fixed exchange energy and boundary transparency and a different proximity effect strength, are presented in Fig. 6.

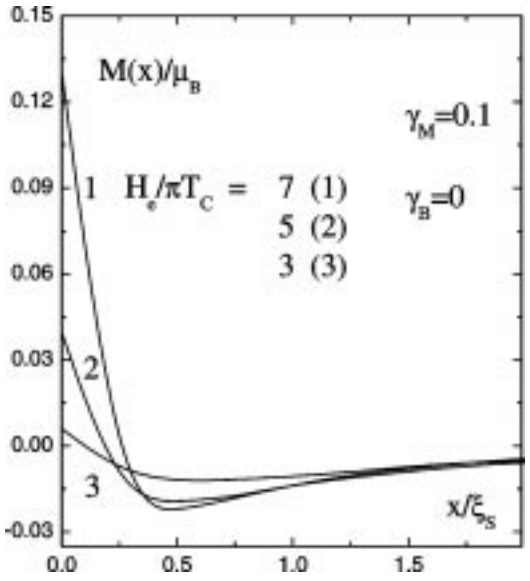


Fig. 5. Leakage of magnetization into the S material versus distance from the interface for an SF sandwich for $\gamma_M = 0.1$, $\gamma_B = 0$ and different exchange energies $H_e/\pi T_C$ =7, 5, and 3 (curves *1*, *2*, and *3*, respectively)

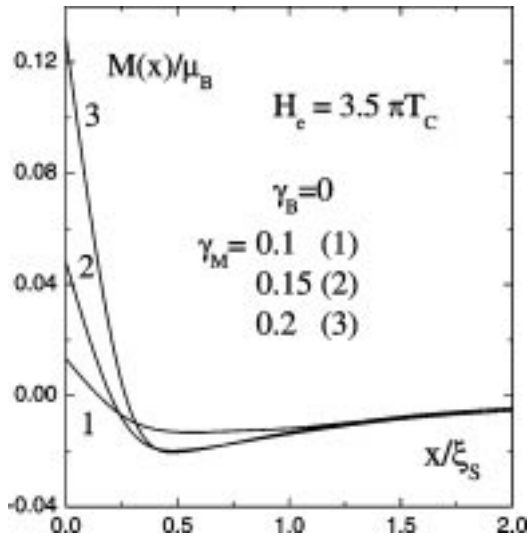


Fig. 6. Same as in Fig. 6 for $\gamma_B = 0$, $H_e = 3.5\pi T_C$ and different proximity effect strengths $\gamma_M = 0.1$, 0.15, and 0.2 (curves *1*, *2*, and *3*, respectively)

### *3.5. Experiment*

There are only a few experimental reports devoted to the questions discussed here. The interplay between magnetism and superconductivity in Nb/Co multilayers was recently investigated in [32]. The upper critical fields of samples were measured for the fields applied in parallel to the plane $H_{C_2||}$ and perpendicularly to the plane $H_{C_2\perp}$ of the films. The effective thickness of the Co layer, $d_{\text{eff}}$ , is defined through the well-known relation

$$d_{\text{eff}} = \left(\frac{\Phi_0}{2\pi H_{C_2\perp}}\right)^{1/2} \frac{H_{C_2\perp}}{H_{C_2\|}},$$

where $\Phi_0$ stands for a flux quantum. Experiments revealed that the effective thickness of the magnetic layer in Nb/Co structures is usually much larger than its physical thickness $d_{\text{Co}}$. For example, taking the data on a sample with $d_{\text{Co}} = 1.8$ nm, the authors obtained $d_{\text{eff}} = 12$ nm, so that $d_{\text{eff}} \gg d_{\text{Co}}$. The 'increase' of the thicknesses was so great that in all samples except for those with extremely thin magnetic layers, the crossover to a 3D state superconductivity is never in fact observed experimentally. This is to be contrasted with the case of nonmagnetic spacer layers, where these two length scales are comparable. Taking into account our results, we explain a rise of the effective magnetic layer thickness in the Nb/Co multilayer as an impact of the proximity effect. Namely, the induced magnetic correlation into the *S* layer depletes the density of Cooper pairs at the SF boundary, which results in an excess thickness of the magnetic layer.

The modification of the DOS in mesoscopic superconducting strips of Al under the influence of the magnetic proximity effect of a classical ferromagnet Ni has also been studied both theoretically and experimentally in [33]. However, since the tunnel spectroscopy experiments were carried out with a nonmagnetic probe, the authors cannot measure the spin-dependent local DOS on the superconducting side.

The interest in the magnetic proximity effect has been increased with the development of experimental techniques like neutron reflectometry and muon spin rotation, which allow one to accurately determine the spatial distribution of magnetic moments. For example, the multilayered system $YBa_2Cu_3O_7/La_{2/3}Ca_{1/3}MnO_3$ have been studied very recently by neutron reflectometry in [34]. The evidence for a characteristic difference between the structural and magnetic depth profiles is obtained from the occurrence of a structurally forbidden Bragg peak in the ferromagnetic state. The authors discussed the results in two possible scenarios: a sizable magnetic moment within the S layer antiparallel to that in the F layer (the inverse proximity effect) or a "dead" region in the F layer with zero net magnetic moment.

## 4. Conclusion

In the recent years, the advances in growth and fabrication techniques for materials have made it possible to create heterostructures with high-quality interfaces. Taking into account that ferromagnet-superconductor hybrid systems have great scientific importance and are promising for the application in spin-electronics, it is not surprising that the interest in these hybrid materials has been renewed. As far as the thickness of superconducting and magnetic metals in such structures may be a few atomic periods, the understanding of how the proximity effects modify the electronic properties of S/F interfaces is growing in importance.

We have studied the magnetic correlations acquired by a superconductor at the S/F interface due to a proximity effect. We have found that the equilibrium exchange of electrons between the F and S metals results not only in the proximity-induced superconductivity of the F metal, as was found earlier, but in the proximity-induced magnetism of the S metal, as well. The magnetic correlations spread over a large distance which is of the order of the superconducting coherence length $\xi_S$ and can exceed both the ferromagnetic and the superconducting films thicknesses. That is why the existence of these magnetic properties of the S metal is quite important for SF nanoscale structures and should be taken into account while comparing theoretical results with experimental data. Summarizing the results, we should stress that, for SF nanoscopic hybrid structures, both the superconducting and magnetic proximity effects take place simultaneously.

We wish to dedicate this paper to V.G. Bar'yakhtar, our Master who played a significant exceptional role in our post-student life, on the occasion of his 75th birthday, and to wish him the continuing health and vigour in pursuing his scientific interest. The authors would like to thank V.V. Ryazanov, A.I. Buzdin, L. Tagirov, and M.A. Belogolovskii for the valuable discussions of some questions concerning the proximity effect phenomena. We also acknowledge E.A. Koshina for performing the numerical calculations.

1. *Wolf E. L.* Principles of Electron Tunneling Spectroscopy. — Oxford: Univ. Press, 1985.
2. *Golubov A. A., Kupriyanov M. Yu., Il'ichev E.* //Rev. Mod. Phys. — 2004.— **76**, N2.— P.411—469.
3. *Izumov Yu. A., Proshin Yu. N., Khusainov M. G.* //Usp. Fiz. Nauk. — 2002.— **45**, N2.— P.114—154.
4. *Buzdin A. I., Bulaevskii L. N., Panyukov S. V.* //Sov. Phys. JETP Lett. —1982.— **35**, N4. — P.147—148.
5. *Buzdin A. I., Kupriyanov M. Yu.* //Ibid. — 1991.— **53**, N6.— P.308—312.
6. *Ryazanov V. V., Oboznov V. A., Rusanov A. Yu. et al.* //Phys. Rev. Lett. — 2001.— **86**, N11—12.— P.2427—2430.
7. *Ryazanov V. V., Oboznov V. A., Veretennikov A. V., Rusanov A. Yu.* //Phys. Rev. B. — 2002 — **65**, N2. — 020501-4(R).
8. *Blum Y., Tsukernik A., Karpovski M., Palevski A.* //Phys. Rev. Lett. — 2002. — **89**, N18.— P.187004-4.
9. *Kontos T.,Aprili M., Lesueur J. et al..* //Phys. Rev. Lett. — 2002.— **89**, N13. — 137007-4.
10. *Kontos T., Aprili M., Lesueur J., Grison X.* //Ibid. — 2001.— **86**, N2. — P.304—307.
11. *Guichard W., Aprili M., Bourgeois O. et al.*//Ibid. — 2003.— **90**, N16.— P.167001-4.
12. *Bergeret F. S., Volkov A. F., Efetov K. B.* //Ibid. — 2001.— **86**, N14.— P.3140—3143.
13. *Krivoruchko V. N., Koshina E. A.* //Phys. Rev. B — 2001.— **64**, N17.— P.172511-4.
14. *Golubov A. A., Kupriyanov M. Yu., Fominov Ya. V.* //JETP Lett. — 2002.— **75**, N11.— p.709—713.
15. *Koshina E. A., Krivoruchko V. N.* //Low. Temp. Phys. — 2003.— **29**, N8.— P.642—649.
16. *Halterman K., Valls O. T.* //Phys. Rev. B. —2002.— **65**, N1.— P.014509-12.
17. *Fazio R., Lucheroni C.* //Europhys. Lett. — 1999.— **45**, N6. — P.707—713.
18. *Halterman K., Valls O. T.* //Phys. Rev. B. — 2004.— **69**, N1.— 014517-11.
19. *Krivoruchko V. N., Koshina E. A.* //Ibid. — 2002— **66**, N1.— 014521-6.
20. *Bergeret F. S., Volkov A. F., Efetov K. B.* //Ibid. —2004.— **69**, N17.— P.174504-5.
21. *Millis A., Rainer D., Sauls J. A.* //Ibid. — 1988.— **38,** N7.— P.4504—4515.
22. *Tokuyasu T., Sauls J. A., Rainer D.* //Ibid. — 1988.— **38**, N13.— 8823—8833.
23. *Fogelström M.* //Ibid. — 2000.— **62**, N17.— P.11812—11819.
24. *Usadel K. D.* //Phys. Rev. Lett. — 1970.— **25**, N8.— 507—509..
25. *Swidzinskii A.M.* Spatially Nonuniform Problems of the Theory of Superconductivity. — Moscow: Nauka, 1982 (in Russian).
26. *Koshina E. A., Krivoruchko V. N.*//Low. Temp. Phys. — 2000. — **26**, N2.— P.115—120.
27. *Kupriyanov M. Yu., Lukichev V. F.* //Sov. Phys. JETP — 1988.— **94**, N6.— P.139—149.
28. *Koshina E. A., Krivoruchko V. N.*//Phys. Rev. B — 2001.— **63**, N22.— 224515-8.
29. *DeWeert M. J., Arnold G. B.* //Ibid. — 1989.— **39**, N16.— 11307—11319.
30. *Shiba H.* //Prog. Theor. Phys. — 1968.— **40**, N3.— P.435—451.

31. *Rusinov A.J.* //Sov. Phys. JETP Lett. — 1969.— **9,** N1.— P.85—89.

32. *Ogrin F. Y., Lee S. L., Hillier A. D. et al.* //Phys. Rev. B. — 2000.— **62**, N9.— 6021—6026.

33. *Sillanpää M. A., Heikkilä T. T., Lindell R. K., Hakonen P. J.* //Europhys. Lett. — 2001.— **56**, N4.— P.590—595.

34. *Stahn J., Chakhalian J., Niedermayer Ch. et al.*//Phys. Rev. B. —2005.— **71**, N14 — P.140509-4(R).

## МАГНЕТИЗМ ЧЕРЕЗ НАДПРОВІДНІСТЬ У SF БЛИЗЬКІСТНИХ СТРУКТУРАХ

*В.М. Криворучко, В.М. Варюхін*

Р е з ю м е

Ми розглянули ефекти близькості у гібрідних структурах надпровідник (S) — феромагнетик (F), приділяючи увагу індукованому феромагнетизму S-металу. Аналіз оснований на квазікласичній теорії ефекту близькості для металів у "грязному" наближенні. Показано, що нижче температури надпровідного переходу феромагнітні кореляції проникають у надпровідник на відстань порядку надпровідної довжинии когерентності $\xi_S$ і залежать від параметрів S/F-межі. Наведено аргументи на користь того, що властивості мезоскопічних SF гібрідних систем можуть суттєво залежати від магнітного ефекту близькості, і останні експерименти, що підтримують модель тісної взаємодії надпровідних та магнітних властивостей у SF-структурах.

## МАГНЕТИЗМ ЧЕРЕЗ СВЕРХПРОВОДИМОСТЬ В SF БЛИЗОСТНЫХ СТРУКТУРАХ

*В.Н. Криворучко, В.Н. Варюхин*

Р е з ю м е

Мы рассмотрели эффекты близости в гибридных структурах сверхпроводник (S) — ферромагнетик (F), уделяя внимание индуцированному ферромагнетизму S-металла. Анализ основан на квазиклассической теории эффекта близости для металлов в "грязном" пределе. Показано, что ниже температуры сверхпроводящего перехода ферромагнитные корреляции проникают в сверхпроводник на расстояние порядка сверхпроводящей длины когерентности $\xi_S$ и зависят от параметров S/F-границы. Приведены аргументы в пользу того, что свойства мезоскопических SF гибридных систем могут существенно зависеть от магнитного эффекта близости, и недавние эксперименты, подтверждающие модель тесной взаимосвязи сверхпроводящих и магнитных свойств в SF-структурах.